Global Scientific JOURNALS

CIVIL ENGINEERING | RESEARCH ARTICLE

Discussion on the technology of controlling thermal crack of mass concrete in the tropics: Experimental, modelling and parametric studies

Md shoag

Abstract: This paper is an experimental investigation and analytical simulation of thermal effects on mass concrete structures in the tropics. A study of the temperature rise of a 1.1 m × 1.1 m × 1.1 m experimental mass concrete block, well instrumented with thermocouples to monitor the temperatures distribution was performed. A validated finite element model was used to predict the temperature development of the hydrating experimental mass concrete block. Thermal stress analysis was performed to give an estimate of stresses induced by the thermal gradient of the concrete block section and the crack index was used to quantify the probability of thermal cracking. The temperature rise during concrete hardening is caused by the hydration of cement paste [6,7]. The heat evolution of concrete is particularly important with regard to mass concrete that used for dams and large foundations in which the maximal temperature may reach even 50-70°C [8,9]A parametric study on the effect of the surface area to volume ratio (SVR) of mass concrete was performed to quantify the maximum allowable thermal gradient as well as the induced thermal stresses that may cause thermal cracks. For SVR less than 0.36, thermal cracks may occur at early ages of concrete strength development in the tropics. Subsequently, thermal cracks occur when the tensile stress reaches the tensile strength of concrete. Researchers of this study developed a new automated curing system, which maintains the gap between the internal temperature and external temperature of a structure below a temperature criterion in order to minimize the thermal cracks of mass concrete. The developed curing method was successfully demonstrated through a mock-up test and a field application. Accordingly, it is concluded that the automated curing system developed in this study can improve the quality of mass concrete structure.

Subjects: Materials Science; Composites; Materials Processing; Civil, Environmental and Geotechnical Engineering; Concrete & Cement; Rock Mechanics; Soil Mechanics; Waste & Recycling; Foundations and Piling; Pavement Engineering

Keywords: mass concrete; hydration; temperature; thermal cracks; finite element model

1. Introduction

Whenever large volume of fresh concrete is poured during the construction of large homogeneous structures such as dams, bridges, water retaining structures and foundations, consideration is always given to the amount of heat that will be generated (Gajda, 2007; Klemczak, 2014). The concrete hy-dration is an exothermic reaction that can produce high amounts of heat during curing, especially in the first few days or weeks after casting (ACI Committee 318, 2005; Lawrence, 2009). This heat pro-duction can produce high temperatures at the centre of the mass concrete due to the insulating effect of the concrete. Since the concrete surface temperatures are lower due to the heat dissipated into the ambient environment, temperature gradients are formed (Khan, Cook, & Mitchell, 1998; Lachemi & Aïtcin, 1997; Lawrence, 2009; Pofale, Tayade, & Deshpande, 2013). These changes in temperature cre-ate volumetric changes, i.e. expansion from heating and contraction from cooling in the concrete (Lin & Chen, 2015; Tia, Lawrence, Ferraro, Do, & Chen, 2013). When these volumetric changes are re-strained by the supports and the more mature interior concrete, tensile stresses are formed on the concrete's surface (Riding, Poole, Folliard, Juenger, & Schinder, 2012). If the surface tensile stresses become higher than overall tensile strength of the concrete, cracking normally occurs (de Borst & van den Boogaard, 1994; Kim, 2010; Lawrence, 2009). The cracking is even magnified in early age concrete that is still developing its full strength (Cervera, Faria, Oliver, & Prato, 2002; Lee & Kim, 2009).

Past research works on the creation of numerical models for the prediction of temperature distribu-tion in mass concrete mainly focused on using basic heat generation functions for the calculation of adiabatic temperature rise (Ballim, 2004; Chini & Parham, 2005; De Schutter, 2002; De Schutter, Yuan, Liu, & Jiang, 2014; Ilc, Turk, Kavčič, & Trtnik, 2009; Tanabe, Kawasumi, & Yamashita, 1986; van Breugel, 1991). The used of real measured heat of hydration results from calorimetry testing of the cement paste is mostly uncommon in Africa, especially Ghana due to the initial cost in acquiring the instruments- (Kim, 2010; Milestone & Rogers, 1981). However, available literature reviews that numerous labs in North America and Europe have calorimeter(s) for measuring the real heat of hydration (Cao, Zavaterri, Youngblood, Moon, & Weiss, 2014). Instead, attempts at modelling hydrating mass concrete have treated the heat generated by the reacting cement as being uniform throughout the concrete mass. Whereas, in reality, the heat generation is a function of the temperature and time history of the -concrete at individual locations in the concrete mass (Lawrence, 2009; Radovanovic, 1998).

Although the effects of thermal gradients on mass concrete is well known in developed countries, there is no agreed maximum allowable temperature differential value between the centre of a mass concrete element and its surface. Bobko, Edwards, Seracino, and Zia (2015), have modelled the ther-mal behaviour of hydrating mass concrete with some degree of success and have fixed the tempera-ture differential at 20°C (35°F). However, in the country where this temperature differential value was developed, a several agencies have established their own guidelines to regulate and control the adverse effect of thermal cracking in mass concrete depending on the time and location where such massive concrete projects are taking place (Edwards, 2013; Lawrence, Tia, Ferraro, & Bergin, 2012; Lawrence, 2009). This confirms the fact that heat generation in mass concrete structures varies for the tropics and the temperate zones for the same type of cement (Do, Lawrence, Tia, & Bergin, 2015). But in the tropics, specifically Ghana, these values do not even exist. This paper therefore formulated a finite element model, taking into consideration the non-homogeneity of heat genera-tion within the mass concrete, the resulting thermal gradients, the associated thermal stresses and strains, and how to accurately predict the distribution of temperature in a hydrating concrete mass in the tropics. Novelty of this work is the developed finite element analysis model that can be used by agencies to predict the temperature distribution and the associated stress development in mas-sive concrete structures in the tropics.

2. Thermal stresses

The thermal stresses that occur during the hardening of mass concrete are extremely complex and difficult to measure. This is due to several factors, chief among which is the complex distribution of temperature changes throughout the volume of the mass concrete. The central region of the mass concrete at early age experiences high but uniform temperatures while the temperature in the outer region decreases as we move closer to the surface (Folliard et al., 2008). Since the maturity of concrete and strength are functions of temperature, the central region of the mass concrete structure will be matured and stronger than the outer region. As the concrete hydrates faster in the middle, large thermal gradients are produced, and strength and maturity are decreased moving outwards towards the surface. Restraint against this contraction will cause tensile stresses and strains to de-velop, creating the possibility for cracks to occur at or close to the surface of the concrete (Atrushi, 2003; Yuan & Wan, 2002). These cracks are initiated when the tensile stresses exceed the low tensile strength at the surface. The magnitude of the tensile stresses are dependent on the difference in the mass concrete, creep or relaxation of the concrete, the coefficient of thermal expansion, the degree of restraint in the concrete and elastic modulus. The development of cracks will affect the ability of the concrete structure to withstand its design load, and further allow the infiltration of lethal materi-als which will undermine the integrity and durability of the mass concrete structure (De Schutter et al., 2014; Lawrence, 2009; Lawrence et al., 2012).

The causes of early age thermal cracking may include either internal or external restraint (ACI Committee 207, 2005a; Kim, 2010). Internal restraint is brought about by strain gradients within the material while exterior restraint is brought about by externally applied loads. This degree of restraint varies between 0 and 100% depending on the physical boundary conditions and on the geometry of the structure (Muhammad, 2009). To accurately predict these thermal cracks, thermal properties that need to be modelled include the specific heat, the coefficient of thermal expansion, thermal diffusivity and heat production. Mechanical properties that need to be quantified, in order to simu-late a finite element model of the experimental block include the tensile strength, tensile strain and elastic modulus (Atrushi, 2003; Gawin, Pesavento, & Schrefler, 2006a, 2006b; Ulm & Coussy, 1995).

According to de Borst and van den Boogaard (1994), Ishikawa (1991), Jaafar (2007), Lawrence et al. (2012), Noorzaei, Bayagoob, Thanoon, and Jaafar (2006), and Tang, Millard, and Beattie (2015), Finite Element Method (FEM) which is a numerical modelling method is seen as the best predictor of thermal cracks in concrete. It offers a step-by-step approach in solving the problem though it has its own limita-tions of been costly and impossibly used at site to quickly determine the maximum heat of hydration of concrete (De Freitas, Cuong, Faria, & Azenha, 2013; Tatro & Schrader, 1992; Zhai, Wang, & Wang, 2015).

3. Experimentals—materials and methods

3.1. Concrete mix design (sample preparation)

The two concrete mixes used in this study had a water to cement ratio of 0.42 to allow for complete hydration. Both concrete mixes had 100% Type I Portland cement concrete. The concrete mix designs evaluated in this paper were prepared manually by mixing Type I Portland cement concrete, water, sand (quarry dust) and 20 mm machine crushed aggregates to obtain mixes 1 and 2 using design mix ratios in Table 1. Equipment used were strain gauges, loading fame, signal conditioning

Table 1. Mix designs of concrete used in the large-scale blocks

Materials	Mix 1	Mix 2
Cement	485 Kg	500 kg
Sand: quarry dust (1:1)	762 Kg	740 Kg
Aggregates (20 mm) (machine crushed)	1,009 Kg	1,031 Kg
Design mix ratio	1:2:4	1:2:4
Water (w/c = 0.42)	204 Kg	210 Kg

Figure 1. Experimental block geometry.

Note: All dimensions in mm.

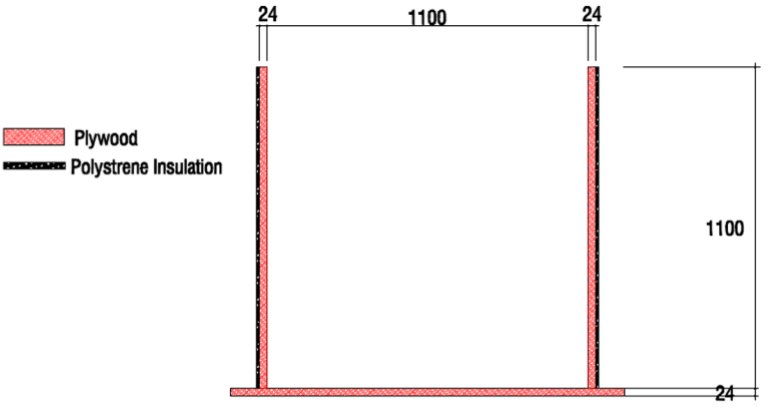

unit, data logger thermocouples and two computers (one for strain and the other for load cell acquisition). Concrete mix 2 was assumed to be fully adiabatic while mix 1 was assumed to be semi adiabatic. The semi adiabatic mix actually simulates the existing field practises in the tropics as achieving fully adiabatic is not possible under the prevailing working conditions. The raw materials information is also found in Table 1.

Two mass concrete blocks of dimensions 1.1 m × 1.1 m × 1.1 m were built (Figure 1) using 150 mm × 150 mm × 600 mm beam moulds. Also, a 24 mm thick plywood with a 1 mm layer of polystyrene sheet was used as insulating material for one of the blocks. These blocks were setup to measure the thermal behaviour of concrete under semi adiabatic conditions. However, in an effort to simulate a full adiabatic process a 50 mm thick sand was added to the top surface of the already placed concrete. Figures 2 and 3 are the individual blocks after the concrete had been poured with and without the formwork respectively.

3.2. Instrumentation for data collection

Data logger thermocouples were instrumented at critical positions in the two experimental concrete blocks to monitor the temperature distribution with time. The layout of the thermocouples are presented in Figure 4. The thermocouples data were recorded at various times in order to calibrate the proposed finite element model to be used to estimate the potential for crack-growth in early age mass concrete.

Figure 2. Experimental block with concrete and sand insulation.

Figure 3. Early age concrete block without formwork.

Figure 4. Thermocouple locations in Block 1 and Block 2.

Note: All dimensions in mm.

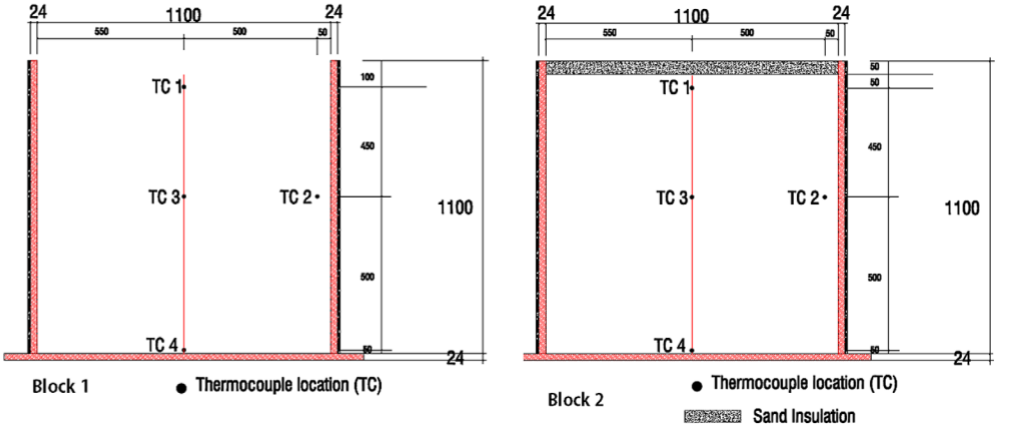

3.3. Temperature profiles

The location of the temperature sensors in the blocks was strategically chosen to capture the differences in temperature between the centre of the block and the exposed surface. The ambient temperature was also monitored to determine if it would contribute to thermal cracking of the concrete. The temperature sensors at the side and bottom of the block were also placed to validate the effectiveness of the insulation, and to also assess the boundary conditions used in the proposed finite element model (Do, Lawrence, Tia, & Bergin, 2014).

3.4. Mechanical properties of concrete

In order to accurately model early-age stress development in concrete members, it was necessary to determine the mechanical properties (Atrushi, 2003; Bernard, Ulm, & Lemarchand, 2003). Many forms of equations have been developed to relate the compressive strength to the maturity development. Two commonly used equations according to Viviani (2005), are given as Equations (1) and (2):

$$f_C(t) = a + b\log(\log(M(t))), \quad f_C \geq 0 \tag{1}$$

$$f_c(T_C) = F_{\text{Cult.}} \exp\left(-\frac{T_E}{\tau_s}\right) \tag{2}$$

where, f_C is the compressive strength value (MPa), a is a fit parameter which is usually negative (MPa), b is a fit parameter (MPa/°C/h), $f_{\text{Cult.}}$ is the ultimate compressive strength parameter fit from the compressive strength tests (MPa), τ_s is a fit parameter (h), T_e is equivalent age at the reference

curing temperature (h), β_s is a fit parameter, $M(t)$ is the maturity or temperature-time factor at age t, tc is average concrete temperature during the time interval, t is time

For thermal stress analysis, Equation (2) was preferred since is not discontinuous at setting and this functional form is similar to hydration models. The fit parameters $f_{Cult.}$, τ_s and β_s were found to be 27.4, 12.35 and 1.52 respectively with an R_2 of 0.98.

In terms of concrete tensile strength, values used for the study were estimated from their respective compressive strengths (Folliard et al., 2008). Most current method for calculating the splitting tensile strength, Equation (3) assumes a power type function based on the compressive strength according to Raphael (1984):

$$f_{Ct} = a(f_c)^b \tag{3}$$

where, f_{Ct} is the concrete splitting tensile strength value, a and b are fit parameters, and f_C is the concrete compressive strength. Fit parameters a and b were found to be 0.06 and 1.09, respectively with an R_2 of 0.99.

Moreover, for accurately modelling of the thermal behaviour (stresses) of mass, it is important to consider the changes in the mechanical properties (elastic modulus) with time of the concrete (De Schutter, 2002; Lawrence et al., 2012). The elastic modulus is also commonly calculated from the concrete's compressive strength. Most models of this type follow a form of Equation (4):

$$E = k(f_C)^n \tag{4}$$

where, E is the elastic modulus, f_C is the compressive strength (MPa), and k and n are model parameters.

Equation (4) was used in calculating the elastic modulus from the compressive strengths developed because most engineers are familiar with it from prior experience in structural design, and readily accept its use.

4. Finite element thermal modelling

The Fourier heat transfer equation is the underline mathematical model can be used to compute the temperature for an elemental volume at a particular instance of time. The generalized governing Equation (5) expressed in the Cartesian coordinate system, was used in the three dimensional heat flow analysis.

$$c_p \frac{\partial T}{\partial t} = k\left(\frac{\partial^2 T}{\partial x^2} + \frac{\partial^2 T}{\partial y^2} + \frac{\partial^2 T}{\partial z^2}\right) + Q_H \tag{5}$$

where, c_p is the specific heat capacity, ρ is the density of the concrete, t is the time, k is the thermal conductivity, T is the temperature and Q_H, the rate of internal heat evolution, x, y, z are the coordinates at a particular point in the structure.

This finite element model that was used to simulate the thermal behaviour in mass concrete was verified or calibrated so that its temperature distribution for the entire volume closely match with that of the experimental block. The main modelling parameters utilized in the thermal analysis were:

- Convection coefficient.
- Ambient temperature.
- Internal heat generation rate of concrete.
- Placing temperature.

4.1. Input parameters for thermal analysis

The input parameters were either modelled as deterministic or stochastic based on the type of analysis, the type of element and the reference temperature, the heat generation function etc. A nonlinear formulation of the transient thermal analysis was adopted to account for the variations of boundary and loading conditions with time. Also, at the element level in the finite element analysis, a utilization of solid elements capable of providing reliable estimates of the thermal quantities were simulated using an eight-node isoparametric element having a single degree of freedom at each node. Under, the ANSYS platform, the PLANE 70–3D thermal solid element type was chosen from the library of constitutive material elements. The main output parameters that were of interest are the maximum in-place temperature and the thermal gradient. We defined thermal gradient as the change in temperature with respect to change in distance across a section of the concrete. Since the thermal properties for an elemental volume changed with time, coupled with convection at the surface above the formwork, an initial boundary temperature referred to as the reference tempera-ture was chosen as the placing temperature. This parameter needed to be defined so that the time-stepping algorithm be initiated in the analysis.

4.2. Poisson's ratio

According to Mehta and Monteiro (2013), Poisson's ratio has no consistent relationship with the curing age of the concrete. A value of 0.18 was used, which was within the universally accepted range of 0.15 and 0.20 for concrete.

4.3. Thermal conductivity

A characteristic value of thermal conductivity of concrete is in the range 9 to 10.5 kJ/mh°C per the Korean standards and in the range 7.1 to 10.6 kJ/mh°C per the American Standards (ACI Committee 207, 2005b). A constant thermal conductivity value of 9 kJ/mh°C was adopted in this study per the assumption that it will not vary with location across a section, and time during the analysis.

4.4. Specific heat of concrete

A typical value of specific heat capacity for concrete ranges from 1.13 to 1.3 kJ/kg°C according to JCI, and 0.92–1.00 kJ/kg°C according to ACI Committee 207 (2005b). The specific heat values chosen in this study are 0.9 kJ/kg°C

4.5. Coefficient of thermal expansion

The coefficient of thermal expansion used in this thermal stress analysis was $2 \times 10_{-6}$/°C.

4.6. Initial boundary conditions consideration

Boundary heat transfer conditions, which are time or temperature dependent, are important for solving the Fourier differential equations. The four major boundary heat transfer mechanisms are conduction, convention, solar absorption, and irradiation. Each point of a concrete element has a different rate of heat of hydration due to the effects of the environment. We considered the overall convection heat transfer caused by air motion using Newton's law of cooling (Equation (6)).

$$Q = hA(T_S - T_a) \tag{6}$$

where, Q is heat flow (kJ/h), h is mean convection heat transfer coefficient (kJ/m$_2$ h°C), A is surface area (m$_2$), T_S is surface temperature (°C), T_a is air temperature (°C).

The combined heat transfer coefficient used to account for convection as well as irradiation throughout the thermal analysis was 29.3 kJ/m$_2$h°C.

4.7. Modelling of heat of hydration from cementitious material

The discrete time-dependent temperature profile at the core of the experimental block was used to predict a continuous heat of cement hydration in the modelling. Due to the nature of the heat curve, the adiabatic hydration model that is usually defined by exponential function has been proposed by

a number of researchers. The empirical adiabatic hydration model proposed by Suzuki, Tsuji, Maekawa, and Okamura (1990) was used to relate the rate of heat evolution of the cementitious material. Equation (7) was used to compute internal heat evolution to define the temperature rise curve.

$$T_a(t) = T_\infty \ 1 - e^{-t} \tag{7}$$

where, T_∞ is the ultimate temperature rise, $T_a(t)$ is the Adiabatic temperature rise at t days after casting, α is the coefficient of temperature rise (reaction rate), t is time in days.

4.8. Modelling of heat generating rate

The time—dependent temperature distribution at the core of the concrete block was used to simulate adiabatic temperature rise. These temperature were then normalized by subtracting the initial placing temperature. Suzuki's model was adopted, by which a univariate nonlinear regression analysis was performed to establish the temperature—time relationship. The software package MATLAB was used to perform this analysis. Upon comparing the predicted model with experimentally determined results at a 95% confidence interval, R_2 Value of 0.988 was obtained. The proposed model quantified the volumetric for the thermal analysis using Equation (8):

$$q(t) = 20{,}000 \times E^{\left(-0.9398^{-\frac{t}{24}}\right)} \tag{8}$$

where, $q(t)$ is the heat generation per unit volume in t days, t is time in days.

4.9. Model geometry

A 1.1 m × 1.1 m × 1.1 m finite element model of the experimental block was constructed in the software package, ANSYS. A mass concrete block was then used to measure the effect of the heat evolu-tion rate on the temperature development with time and location. A discretization scheme of 50 mm along each edge of the block was chosen while a temperature based convergence criteria was set to give reliable estimates of the temperature distribution. The element type concrete 65 was used to represent the element definition to produce 10,648 elements and nodes that were meshed in other to solve the problem. Figure 5 shows the ANSYS model block and Table 2 shows the summarised input parameters values used in the analysis.

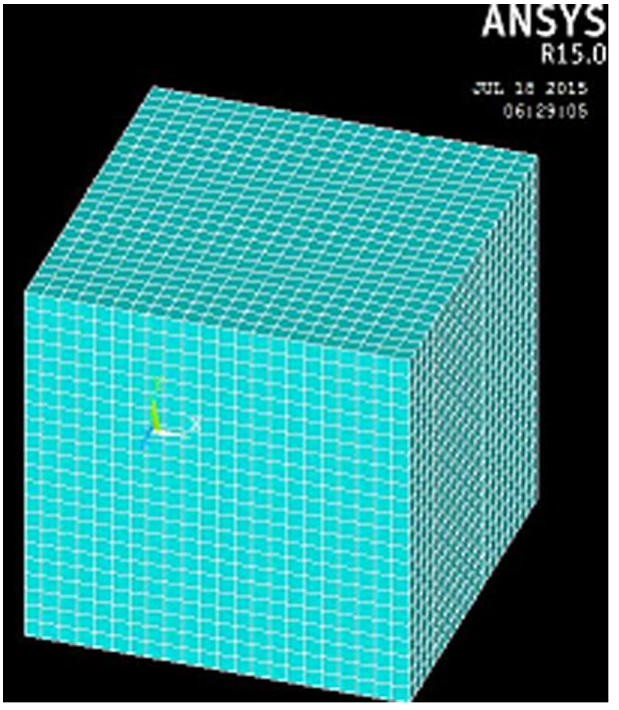

Figure 5. Analytically modelled block of mass concrete.

Table 2. Execution parameters used for both thermal analysis and stress analysis

Items	Unit	Value
Specific heat	kJ/kg/°C	0.96
Thermal conductivity	kJ/mh/°C	9
Thermal expansion	°C	2×10^{-6}
Poisson's ratio	Unitless	0.18
Placement temperature	°C	31.8
Analysis time	h	144
Convection (Plywood form)	$kJ/m_2h°C$	29.3
Density	kg/m_3	2,400

The transient thermal analysis model was implemented in the commercial finite element pro-gram, ANSYS, a general purpose program capable of numerical simulation of a variety of physical problems. For concrete structures with surface area to volume ratio (S_v) being less than 2, it can be classified as massive and as such the thermal effect should be considered (Flaga, 2011). Thus, we simulated analytically the specified heat generation rate, mechanical and thermal properties of the experimental block of concrete having geometric configuration of 1.1 m × 1.1 m × 1.1 m and S_v of 0.91. The parameters that were treated mainly as random variables were the ambient temperature, the hydration rate of the cementitious material as well as the heat transfer coefficient for the differ-ent surfaces of the mass concrete block. The ambient temperature and the heat evolution from the hydrating cement played major roles in the temperature rise in mass concrete (Ayotte, Massicote, Houde, & Gocevski, 1997; Truman, Petruska, Ferhi, & Fehl, 1991). Though these variables were ran-dom in nature, the temperature distribution at that particular time was assumed to emanate from a stochastic process. Also, because strength properties of concrete increased with time, coupled with the large thermal gradient between the core and surface of a mass concrete section, the dam-aging effect of the thermal behaviour of the hydrating cement was considered critical at early age.

We defined early age of mass concrete as the first 6 days after placing of concrete. Therefore, the transient thermal analysis was estimated for 6 days. In order to monitor the temperature distribu-tion with respect to time, the experimental concrete block was well instrumented with thermocou-ples at specific location (Figure 4). Measurements were then taken at discrete time steps of 2, 12, 18, 24, 48, 72, 96, 120 and 144 h.

5. Validation of analytical model

Figure 6 shows the analytical output of the temperature variation at the centre of the concrete block. Spline interpolation was adopted in order to obtain a continuous function of the time-temperature development. Figure 7 shows comparatively results of the observed temperature distribution and the simulated analytical results at the core of the concrete. A 75.4°C temperature rise at 24 h was observed at the core of the mass concrete section considered, with a gradual decline to 40.36°C at 144 h after placing of concrete. A temperature rise of 75.4°C meant that there was Delayed Ettringite Formation (DEF) which led to massive cracking of the experimental blocks (Gajda & Vangeem, 2002). Other contributing factors of the DEF development may include; temperature, alkalis in the cement, SO_3 and C_3A contents of the cement, aggregate mineralogy, and high humidity conditions (Loïc, 2003). The value of 75.4°C is comparable to temperature rise within 24 h of concrete placement value of 74.32°C obtained by Prasanna and Subhashini (2010), and the range of 79 to 42°C obtained by Bartojay (2012). A maximum temperature differential at a particular instant of time was 22.9°C throughout the analysis period (observed at the core and surface of the concrete block). This differ-ence is attributed to the fact that hydrating concrete at the surface loses heat to the atmosphere at a higher rate than the core element of concrete.

Figure 6. Temperature variation at the Centre of the concrete block.

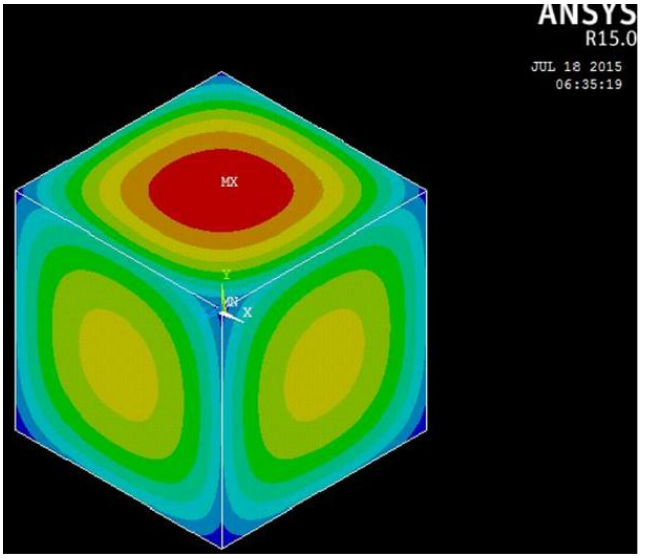

Figure 7. Temperature variation at the core of the concrete block with respect to time.

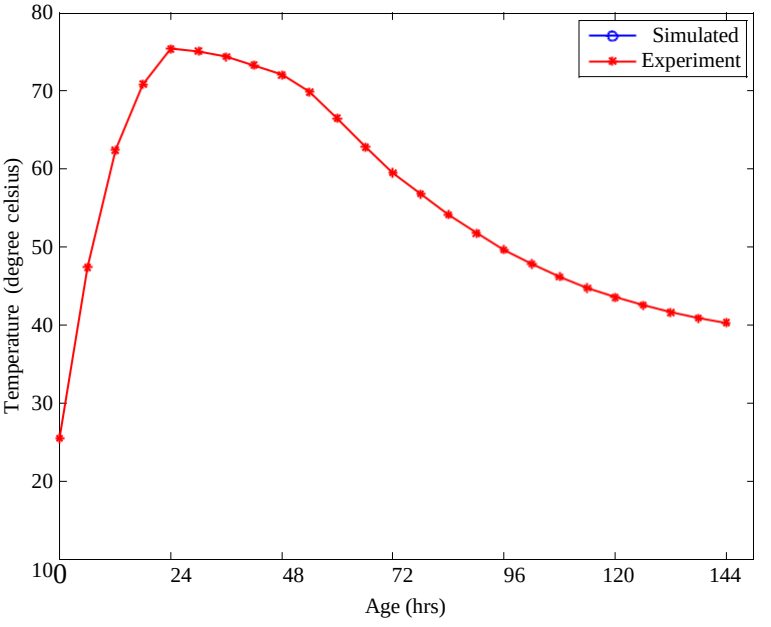

6. Thermal stress analysis

The temperature distribution and the thermal gradient are primarily the thermal quantities that were of interest in our transient thermal analysis model (Khan et al., 1998; Waller, D'Aloïa, Cussigh, & Lecrux, 2004). However, to actually ascertain the potential for cracking due to this external state of loading, a stress analysis was required to assess whether the limiting state of stress has been exceeded. The limit state condition occurred when the thermally induced stresses were greater than the tensile strength of concrete at a given age. Internal restraints caused the maximum tempera-ture differential, the uneven expansion and the contraction of the two extremes for a given section, thereby producing cracks at the upper surfaces (Khan et al., 1998; Lachemi & Aïtcin, 1997). The procedure adopted for the stress analysis is similar to that of the thermal model. Definitions of ele-ment type, analysis type and quantification of the variations in mechanical properties and boundary conditions were made. The temperature distribution over the entire concrete block was applied as load in this model at every time step.

Figure 8. Stress analysis results.

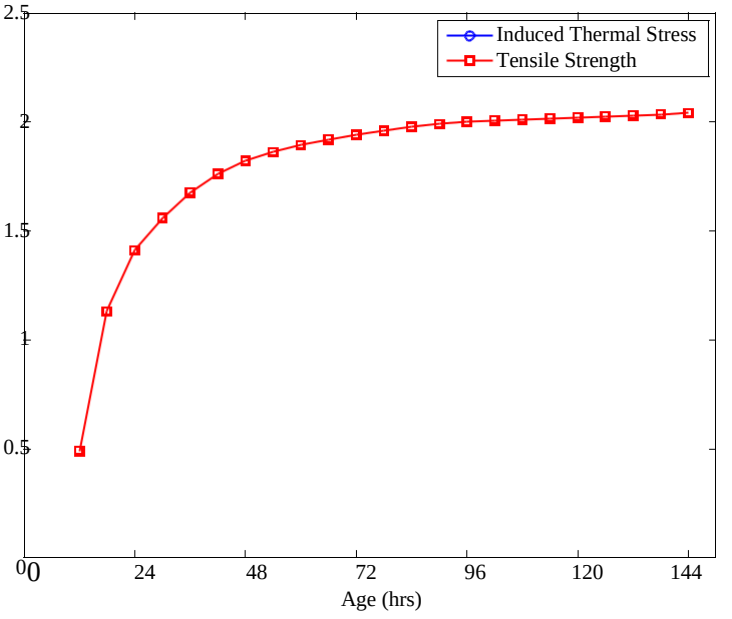

6.1. Thermal stress analysis results

Figure 8 presents the results of thermal stress analysis for the analytical model. The maximum tensile stress in all the orthogonal directions, due to thermal distribution was found to occur around the surface. The maximum thermal stresses coincided with the time corresponding to the peak temperature distribution. For the validated analytical model, it occurred at 24 h after placing concrete. Beyond this time, there was a gradual decline in the thermal stress because the corresponding temperature development was also decreasing. Due to this phenomenon, the temperature at early age was key in estimating the occurrence of cracks in mass concrete. The crack index, defined as the ratio of tensile strength of concrete to the induced thermal stress at early ages, was used to measure the probability of cracks developing in the mass concrete structure. For crack index values less than unity, thermal crack is expected to occur. The validated analytical model yielded a crack index value of 2.1 signifying that stress induced by the temperature development were not large enough to cause thermal cracks.

7. Parametric study and probabilistic prediction of thermal crack

7.1. Effect of specimen size

The standard specimen size used in this study was a block size of 1.1 m × 1.1 m × 1.1 m. To study the effect of size on the behaviour of concrete, four additional block sizes were modelled. The sizes cho-sen were: 2 m × 2 m × 2 m, 3 m × 3 m × 3 m, 4 m × 4 m × 4 m and 5 m × 5 m × 5 m. A comparison of the temperature profiles at the centre of blocks containing concrete is shown in Figure 9. The surface area to volume ratio of each specimen was used as a parameter to evaluate the temperature distri-bution. It is evident that as the surface area to volume ratio decreased, there was a corresponding increase in temperatures with respect to time of each specimen.

Also, Figure 9 shows the progression of the peak temperatures, as the surface area to volume ratio decreased (indirectly increased in block size). It has been observed that, mass concrete structures with peak temperatures higher than 70°C are expected to experience an undesirable phenomenon known as DEF (Kishi & Maekawa, 1995; Lawrence, 2009; Tim, 2014; Wang, Ge, Grove, Ruiz, & Rasmussen, 2006). From Figure 9, surface area to volume ratios for all the specimens under study yielded a maximum observed temperature rise exceeding 70°C.

Figure 9. Comparison of temperature profiles calculated at the centre of each block.

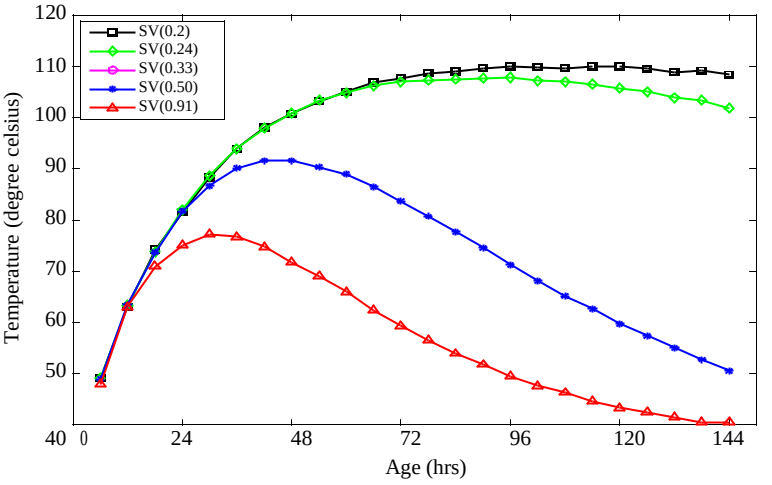

Figure 10. Calculated peak temperature values with respect to block size.

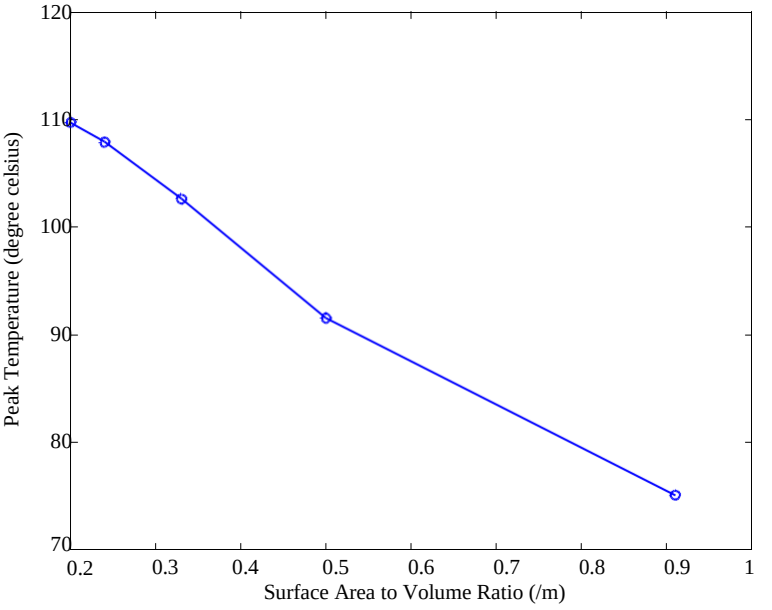

The effect of the surface area to volume ratio (indirectly the block size) on the maximum temperature differentials is presented in Figure 10. The maximum temperature differential between the centre and top surface edge increased from 22.9°C in the 1.1 m block to 70.1°C for the 5 m block. The temperature differentials and the thermal gradient (change in temperature with respect to distance) were the major parameters used to measure the degree of internal restraint caused by the temperature rise in mass concrete. The maximum temperature differential limiting value of 20°C was assumed between the surface and centre of mass concrete structure to achieved desirable strength characteristics with no thermal crack. From Figure 10, both the experimental and the analytical results produced temperatures higher than 20°C for all the specimens under study. A univariate regression analysis revealed Equation (9):

$$T_{MAX} = 76.144\, S_V^{-0.24149}, \text{ WITH } R^2 \text{ VALUE OF } 0.957 \quad (9)$$

where, T_{max} is the maximum temperature differential, S_v is the surface area to volume ratio.

Figure 11. Maximum induced stress with respect to maximum temperature differential due to increasing block size.

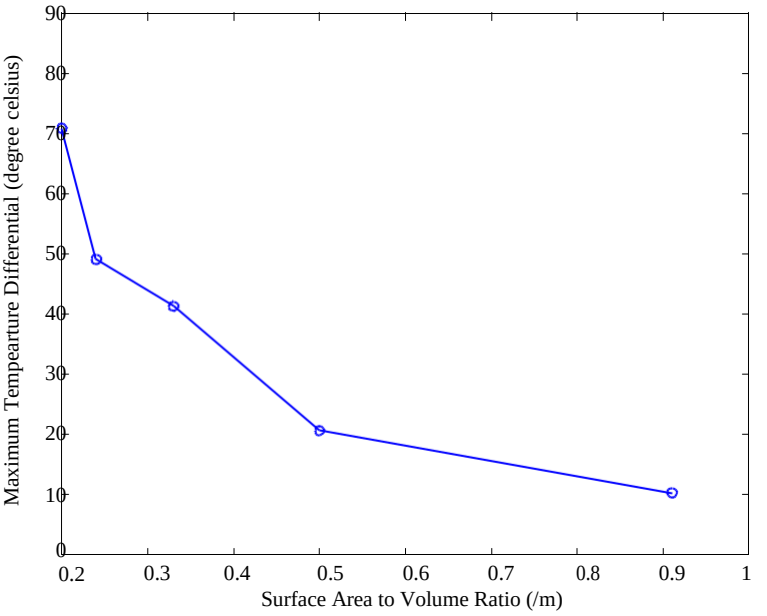

The relationship between the maximum induced stress and the increasing maximum temperature differential caused by increasing block size (decreasing surface area to volume ratio) is presented in Figure 11. For a given concrete mixture, the maximum induced stress increased with increasing maximum temperature differential (correlation coefficient of 0.99). Also, the maximum temperature difference and resulting stress in concrete elements were highly dependent on the type of concrete used.

Figure 12 shows a propagation of maximum induced stress with respect to surface area to volume ratio. When these stresses are higher than the tensile strength, thermal crack may occur. Superimposed on Figure 12 is the tensile strength for the various specimen under study at times when the thermal stresses are expected to be maximum. It was revealed that at surface area to volume ratio roughly higher than 0.36, thermal crack may not be observed. A univariate nonlinear regression was done to provide a relation between both quantities as provided in Equations (10) and (11).

$$\sigma_{TENSILE} = 1.4726\, S_V^{-0.2209}, \text{ WITH } R^2 \text{ VALUE OF } 0.867 \quad (10)$$

Figure 12. Maximum induced stresses to the Surface area to volume of each block.

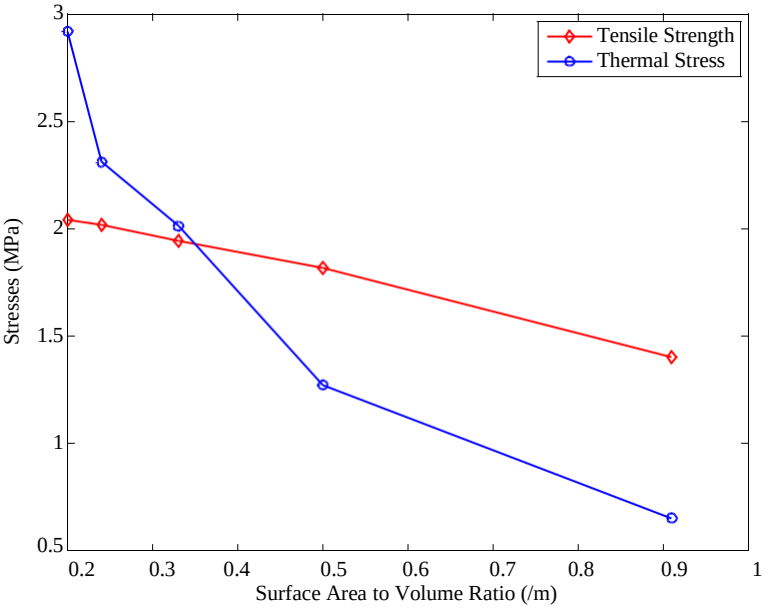

Figure 13. Crack Index to the surface area to volume ratio of each block.

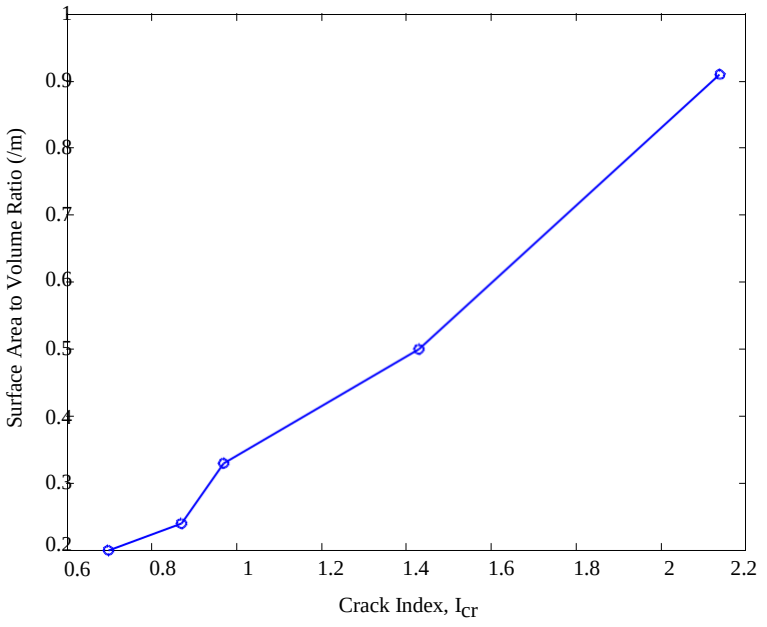

$$\sigma_{THERMAL} = 0.68192\, S_V^{-0.89648}, \text{ WITH } R^2 \text{ VALUE OF } 0.976 \quad (11)$$

where, $\sigma_{tensile}$ is the tensile strength, $\sigma_{thermal}$ is the thermal stresses, S_v is the SVR.

Figure 13 relates the crack index to the surface area to volume ratio. It can be seen that these two parameters are highly correlative (R_2 value 0.992). For surface area to volume ratio less than 0.36, the crack index was less than 1, signifying that the induced thermal stresses have exceeded the tensile strength at that concrete age, therefore the probability of thermal cracks developing become certain. The regression analysis yielded Equation (12):

$$I_{CR} = 2.2982\, S_V^{0.72216}, \text{ WITH } R^2 \text{ VALUE OF } 0.992 \quad (12)$$

where, I_{cr} is the crack index, S_v is the SVR.

8. Conclusions

Investigations were conducted on predicting early age thermal cracks in mass concrete structures at tropical atmospheric conditions using Ghana as the geographical scope for the research. The current state-of-the-art practice is to perform adiabatic calorimetry testing on concrete mixtures and use fi-nite element analysis to predict temperature distribution during the time. The predicted temperature distribution is then used to quantify the induced thermal stresses. Given that the tensile strength at a particular age of concrete is less than the thermal stress, the probability of thermal cracks developing becomes certain. The research adopted both experimental and analytical modelling (Finite Element Model) scenarios to predict the early age thermal cracking in mass concrete structures in the tropics. The experimental program involved the construction of two mass concrete blocks of dimension 1.1 m × 1.1 m × 1.1 m that were intended to simulate both adiabatic and semi adiabatic conditions. The temperature distributions from these experimental blocks were used to calibrate and validate fi-nite element models that were implemented in the commercial software ANSYS. A parametric study on the effect of the size on various concrete blocks were also investigated to help estimate the propa-gation of crack growth during the early ages of mass concrete structures. From the study, construc-tion of mass concrete structures with SVR less than 0.36 is not adequate enough to prevent the occurrence of cracks. Also, the age of concrete at peak temperature was observed to increase with an increase in the size of the mass concrete block. The specific conclusions drawn were:

(1) The widely accepted limiting temperature differential of 20°C that is likely to cause thermal cracking may not be valid in the tropics for mass concrete structures.
(2) In the tropics mass concrete structures with a SVR value less than 0.36 are expected to cause thermal cracking at early ages of cement hydration.
(3) As such to provide reliable estimate of the likelihood of cracking, this assertion should be supplemented by performing a finite element stress analysis.
(4) In the tropics, we recommend a minimum of 5 days for de-shuttering of the formwork to prevent the occurrence of thermal shock.

List of Abbreviation for symbols

f_C	compressive strength value (MPa)
a	fit parameter which is usually negative (MPa)
b	fit parameter (MPa/°C/h)
$f_{Cult.}$	ultimate compressive strength parameter fit from the compressive strength tests (MPa)
τ_s	fit parameter (h)
Te	equivalent age at the reference curing temperature (h)
β_s	fit parameter
$M(t)$	maturity or temperature-time factor at age t average concrete temperature -during the time interval
t	time
f_{Ct}	concrete splitting tensile strength value
E	elastic modulus
f_C	compressive strength (MPa)
n	model parameter
c_p	specific heat capacity
ρ	density of the concrete
k	thermal conductivity
T	temperature
Q_H	rate of internal heat evolution
x, y, z	coordinates at a particular point in the structure
Q	heat flow (kJ/h)
h	mean convection heat transfer coefficient (kJ/mh°C)
A	surface area (m_2)
T_S	surface temperature (°C)
T_a	air temperature (°C)
T_∞	ultimate temperature rise
$T_a(t)$	Adiabatic temperature rise at t days after casting
α	coefficient of temperature rise (reaction rate)
$q(t)$	heat generation per unit volume in t days
T_{max}	maximum temperature differential
$\sigma_{tensile}$	tensile strength
$\sigma_{thermal}$	thermal stresses
S_v	surface area to volume ratio
I_{cr}	crack index

Author details

[1] Jiangsu University of Science & Technology, Zhenjiang, Jiangsu, China

References

ACI Committee 207. (2005a). *Guide to mass concrete, ACI 207.1R-05*. Farmington Hills, MI: American Concrete Institute.

ACI Committee 207. (2005b). *Report on thermal and volume change effects on cracking of mass concrete, 207.2R-07*. Farmington Hills, MI: American Concrete Institute. ACI Committee 318. (2005). *Building code requirements for structural concrete (ACI 318–05) and commentary (318R– 05)*. Farmington Hills, MI: American Concrete Institute.

Atrushi, D. S. (2003). *Tensile and compressive creep of early age concrete: Testing and modelling*. Trondheim: Department of Civil Engineering, The Norwegian University of Science and Technology. URN:NBN:no-3377.

Ayotte, É., Massicote, B., Houde, J., & Gocevski, V. (1997). Modelling the thermal stresses at early ages in a concrete monolith. *ACI Materials Journal, 94*, 577–587.

Ballim, Y. (2004). A numerical model and associated calorimeter for predicting temperature profiles in mass concrete. *Cement and Concrete Composites, 26*, 695–703. doi:10.1016/S0958-9465(03)00093-3

Bartojay, K. (2012). Thermal properties of reinforced structural mass concrete. *Dam Safety Technology Development Program, Bureau of Reclamation, OMB No. 0704-0188*. Denver, CO: U.S. Department of the Interior.

Bernard, O., Ulm, F., & Lemarchand, E. (2003). A multiscale micromechanics-hydration model for the early-age elastic properties of cement-based materials. *Cement and Concrete Research*, 1293–1309. doi:10.1016/S0008-8846(03)00039-5

Bobko, P. C., Edwards, J. A., Seracino, R., & Zia, P. (2015). Thermal cracking of mass concrete bridge footings in coastal environments. *Journal of Performance of Constructed Facilities, 29*, 0401–4171. doi:10.1061/(ASCE)CF.1943-5509.0000664

Cao, Y., Zavaterri, P., Youngblood, J., Moon, R., & Weiss, J. (2014). The influence of cellulose nano crystal additions on the performance of cement paste. *Cement & Concrete Composites, 56*, 73–83. doi:10.1016/j.cemconcomp.2014.11.008

Cervera, M., Faria, R., Oliver, J., & Prato, T. (2002). Numerical modelling of concrete curing, regarding hydration and temperature phenomena. *Computers & Structures*, 1511–1521. doi:10.1016/S0045-7949(02)00104-9

Chini, A. R., & Parham, A. (2005). *Adiabatic temperature rise of mass concrete in Florida* (final report). GainesVille, FL: University of Florida.

de Borst, R., & van den Boogaard, A. H. (1994). Finite-element modeling of deformation and cracking in early-age concrete. *Journal of Engineering Mechanics, 120*, 2519– 2534. http://dx.doi.org/10.1061/ (ASCE)0733-9399(1994)120:12(2519)

De Freitas, T., Cuong, J., Faria, R., & Azenha, M. (2013). Modelling of cement hydration in concrete structures with hybrid finite elements. *Finite Elements in Analysis and Design*, 77, 16–30. doi:10.1016/j.finel.2013.07.008.

De Schutter, G. (2002). Finite element simulation of thermal cracking in massive hardening concrete elements using degree of hydration based material laws. *Computers & Structures, 80*, 2035–2042. http://dx.doi.org/10.1016/S0045-7949(02)00270-5

De Schutter, G., Yuan, Y., Liu, X., & Jiang, W. (2014). Degree of hydration-based creep modeling of concrete with blended binders: from concept to real applications. *Journal of Sustainable Cement-Based Materials*, 1–14, doi:10.1080/21650373.2014.928808

Do, A. T., Lawrence, M. A., Tia, M., & Bergin, M. J. (2015). Effects of thermal conductivity of soil on temperature development and cracking in mass concrete footings. *Journal of Testing and Evaluation, 43*, 1078–1090. doi:https://doi.org/10.1520/JTE20140026

Do, T., Lawrence, A., Tia, M., & Bergin, M. (2014). Determination of required insulation for preventing early-age cracking in mass concrete footings. *Transportation Research Record: Journal of the Transportation Research Board, 2441*, 91– 97. doi:10.3141/2441-12

Edwards, A. J. (2013). *Early age thermal cracking of mass concrete footings on bridges in coastal environments* (Unpublished MSc Graduate Thesis). North Carolina State University, Raleigh.

Flaga, K. (2011). *Shrinkage stresses and surface reinforcement in concrete structures*. Monography 391. Krakow: Cracow Technical University.

Folliard, K. J., Juenger, M., Schindler, A., Riding, K., Poole, J., Kallivokas, L. F. … Meadows, J. L. (2008). *Prediction model for concrete behavior - final report* (No. Report No. FHWA/TX-08/0-4563-1). Austin, TX: Texas Department of Transportation and the Federal Highway Administration.

Gajda, J. (2007). *Mass concrete for buildings and bridges*. Skokie, IL: Portland Cement Association.

Gajda, J., & Vangeem, M. (2002). Controlling temperatures in mass concrete. *Concrete International, 24*, 59–62.

Gawin, D., Pesavento, F., & Schrefler, B. (2006a). Hygro-thermo-chemo-mechanical modelling of concrete at early ages and beyond. Part II: shrinkage and creep of concrete. *International Journal for Numerical Methods in Engineering*, 332–363. doi:10.1002/nme.1636

Gawin, D., Pesavento, F., & Schrefler, B. (2006b). Hygro-thermo-chemo-mechanical modelling of concrete at early ages and beyond. Part I: hydration and hygro-thermal phenomena. *International Journal for Numerical Methods in Engineering*, 299–331. doi:10.1002/nme.1615

Ilc, A., Turk, G., Kavčič, F., & Trtnik, G. (2009). New numerical procedure for the prediction of temperature development in early age concrete structures. *Automation in Construction, 18*, 849–855. doi:10.1016/j.autcon.2009.03.009.Manuscript

Ishikawa, M. (1991). Thermal stress analysis of a concrete dam. *Computers & Structures, 40*, 347–352. http://dx.doi.org/10.1016/0045-7949(91)90360-X

Jaafar, M. S. (2007). Development of finite element computer code for thermal analysis of roller compacted concrete dams. *Advances in Engineering Software, 38*, 886–895. http://dx.doi.org/10.1016/j.advengsoft.2006.08.040

Khan, A. A., Cook, W. D., & Mitchell, D. (1998). Thermal properties and transient thermal analysis of structural members during hydration. *ACI Materials Journal, 95*, 293–300.

Kim, S. G. (2010). *Effect of heat generation from cement hydration on mass concrete placement* (No. Paper 11675) (Graduate Theses and Dissertations). Ames, IA: Graduate College Digital Repository.

Kishi, T., & Maekawa, K. (1995). Multi-component model for hydration heating of Portland cement. *Translation from Proceedings of JSCE, 29*, 97–109.

Klemczak, A. B. (2014). Modeling thermal-shrinkage stresses in early age massive concrete structures – Comparative study of basic models. *Archives of Civil and Mechanical Engineering, 83*, 1–13. doi:10.1016/j.acme.2014.01.002 Lachemi, M., & Aïtcin, P.-C. (1997). Influence of ambient and fresh concrete temperatures on the maximum temperature and thermal gradient in a high performance concrete structure. *ACI Materials Journal, 94*, 102–110.

Lawrence, A. M. (2009). *A finite element model for the prediction of thermal stresses in mass concrete* (Unpublished Ph.D. Dissertation). Gainesville, FL: University of FLorida.

Lawrence, A. M., Tia, M., Ferraro, C., & Bergin, M. (2012). Effect of early age strength on cracking in mass concrete containing different supplementary cementitious materials: Experimental and finite-element investigation. *Journal of Materials in Civil Engineering, 24*, 362–372. http://dx.doi.org/10.1061/(ASCE)MT.1943-5533.0000389

Lee, Y., & Kim, J. (2009). Numerical analysis of the early age behavior of concrete structures with a hydration based microplane model. *Computers & Structures*, 1085–1101. doi:10.1016/j.compstruc.2009.05.008

Lin, Y., & Chen, H.-L. (2015). Thermal analysis and adiabatic calorimetry for early-age concrete members: Part 2. Evaluation of thermally induced stresses. *Journal of Thermal Analysis and Calorimetry, 124*, 227–239. doi:10.1007/s10973-015-5131-x

Loïc, D. (2003). Delayed ettringite formation in massive concrete structures: Summary of studies conducted on deteriorated bridges. *Bulletin Des Laboratories Des Ponts et Chaussées, 4473*, 91–111.

Mehta, P. K., & Monteiro, P. J. M. (2013). *Concrete: Microstructure, properties and materials* (4th ed., pp. 259–264). New York, NY: The McGraw-Hill Education.

Milestone, N. B., & Rogers, D. E. (1981). Use of an isothermal calorimeter for determining heats of hydration at early ages. *World Cement Technology, 12*, 374–380.

Muhammad, A. N. (2009). Simulation of the thermal stress in mass concrete using a thermal stress measuring device. *Cement and Concrete Research, 139*, 154–164.

Noorzaei, J., Bayagoob, K. H., Thanoon, W. A., & Jaafar, M. S. (2006). Thermal and stress analysis of Kinta RCC dam. *Engineering Structures, 28*, 1795–1802. http://dx.doi.org/10.1016/j.engstruct.2006.03.027

Pofale, A. D., Tayade, K. C., & Deshpande, N. V. (2013). Calorimetric studies on heat evolution and temperature rise due to hydration of cementitious materials in concrete using semi-adiabatic calorimeter. *Special Issue for National Conference on Recent Advances in Technology and Management for Integrated Growth 2013 (RATMIG 2013)* (Vol. 2013, pp. 1–7). Retrieved from www.ijaiem.org

Prasanna, W. G., & Subhashini, P. A. (2010). Cracking due to temperature gradient in concrete. *International Conference on Sustainable Built Environment (ICSBE-2010) on 13th to 14th December 2010* (pp. 496–504). Kandy.

Radovanovic, S. (1998). *Thermal and structural finite element analysis of early age mass concrete structures*. Winnipeg, Manitoba: University of Manitoba.

Raphael, J. M. (1984). Tensile strength of concrete. *ACI Journal, 81*, 158–165.

Riding, K. A., Poole, J. L., Folliard, K. J., Juenger, M. C., & Schinder, A. K. (2012). Modelling hydration of cementitious systems. *ACI Materials Journal, 109*, 225–234. Retrieved from http://hdl.handle.net/2009/15459

Suzuki, Y., Tsuji, Y., Maekawa, K., & Okamura, H. (1990). Quantification of hydration-heat generation process of cement in concrete. *Japan Society of Civil Engineers (JSCE), 16*, 111–124.

Tanabe, T., Kawasumi, M., & Yamashita, Y. (1986). Thermal stress analysis of massive concrete. *Seminar Proceedings For Finite Element Analysis of Reinforced Concrete Structures. Tokyo, Japan on 21-24 May 1986*. New York, NY: ASCE.

Tang, K., Millard, S., & Beattie, G. (2015). Early-age heat development in GGBS concrete structures. *Structures and Buildings, 168*, 541–553. doi:10.1680/stbu.14.00089

Tatro, S., & Schrader, E. (1992). Thermal analysis for RCC-a practical approach. In K. D. Hansen & F. G. McLean (Eds.), *Roller compacted concrete III* (pp. 389–406). New York, NY: American Society of Civil Engineers.

Tia, M., Lawrence, A., Ferraro, C., Do, T. A., & Chen, Y. (2013). *Pilot project for maximum heat of mass concrete* (Report number: 00093793). Gainesville, FL: The Florida Department of Transportation.

Tim, C. T. (2014). Challenges and opportunities in tropical concreting. *2nd International Conference on Sustainable Civil Engineering Structures and Construction Materials 2014 (SCESCM 2014)* (pp. 348–355). doi:10.1016/j.proeng.2014.12.193

Truman, K. Z., Petruska, D., Ferhi, A., & Fehl, B. (1991). Nonlinear, incremental analysis of mass-concrete lock monolith. *Journal of Structural Engineering, 117*, 1834–1851. http://dx.doi.org/10.1061/ (ASCE)0733-9445(1991)117:6(1834)

Ulm, F., & Coussy, O. (1995). Modeling of Thermochemomechanical Couplings of Concrete at Early Ages. *Journal of Engineering Mechanics, 121*, 785–794. doi:10.1061/(ASCE)0733-9399(1995) 121:7(785))

van Breugel, K. (1991). Simulation model for development of properties of early-age concrete. In L. Taerwe & H. Lambotte (Eds.), *Quality Control of Concrete Structures – Proceedings of the Second International RILEM/CEB Symposium on June 1991* (pp. 139–151). Ghent, RILEM Proceedings 14: E & FN Spon: London.

Viviani, M. (2005). *Monitoring and modeling of construction materials during hardening* (Doctoral Thesis). Lausanne: Swiss Federal Institute of Technology.

Waller, V. D'Aloıa̋, L., Cussigh, F., & Lecrux, S. (2004). Using the maturity method in concrete cracking control at early ages. *Cement and Concrete Composites*, 589–599. doi:10.1016/S0958-9465(03)00080-5

Wang, K., Ge, Z., Grove, J., Ruiz, J. M., & Rasmussen, R. (2006). Developing a simple and rapid test for monitoring the heat evolution of concrete mixtures for both laboratory and field applications. *Center for Transportation Research and Education, Iowa State University* (Report No. FHWA DTF61-01-00042). Washington, DC: National Concrete Pavement Technology Center.

Yuan, Y., & Wan, Z. L. (2002). Prediction of cracking within early-age concrete due to thermal, drying and creep behavior. *Cement and Concrete Research, 32*, 1053–1059. doi:10.1016/S0008-8846(02)00743-3

Zhai, X., Wang, Y., & Wang, H. (2015). Thermal stress analysis of concrete wall of LNG tank during construction period. *Materials and Structures*. doi:10.1617/s11527-015-0656-9

THANKS FOR BEING WITH ME